Molecular dynamics studies of the interface between a model membrane and an aqueous solution

Kai Nicklas,* Josef Böcker,* Michael Schlenkrich,* Jürgen Brickmann,* and Philippe Bopp‡
*Institut für Physikalische Chemie, Technische Hochschule Darmstadt, D-6100 Darmstadt; and ‡Institut für Physikalische Chemie, Rheinisch-Westfälische Technische Hochschule, D-5100 Aachen, Federal Republic of Germany

ABSTRACT Molecular Dynamics (MD) computer simulation studies are reported for a system consisting of two model membranes in contact with an aqueous solution. The influence of the membrane on the adjacent liquid is of main interest in the present study. It is therefore attempted to make the system sufficiently large to encompass the entire region between bulk liquid and the membranes. The latter are modeled by two-dimensional arrays of COO^- groups with rotational and translational degrees of freedom. The water molecules are represented by the well-tested TIP4P model. The intermolecular potentials are parametrized in terms of Coulomb interactions between partial charges on the molecular frames and empirical, mostly Lennard-Jones (12–6), interactions centered at the atomic positions.

A strong layering of the liquid accompanied by an increase in average water density is found in the vicinity of the membrane. The structural perturbation reaches ~8 Å into the liquid. We discuss the static structure in these layers in terms of atom–atom distance distribution functions and study the average orientation of the water molecule dipoles with respect to the membrane. From the distribution of the ions, we find that <50% of the surface charge of the membrane is neutralized by Na^+ ions in the first layer above the membrane. A simplified model of the adsorption site of the ion on the membrane is developed from the distance distributions. Finally the hydration of the Na^+ in the first adsorbed layer is discussed.

I. INTRODUCTION

Membranes have essential functions in living cells. They are composed of proteins and lipids. The lipids form bilayers, which are the basic structures of membranes, and the proteins are embedded in or attached to these structures. Both proteins and lipids are not at fixed positions but can diffuse. The usually fluid-like dynamics of the membrane (fluid mosaic model) complicates the microscopic description considerably. The structure and the dynamics of the membrane are furthermore influenced by the surrounding medium, which is usually water or an aqueous solution. Vice versa, the membrane will exert a strong influence on the liquid in its vicinity. This is the aspect that we are mostly interested in because this interfacial region is where many chemical reactions of biological importance take place.

The goal of studying in detail a phospholipid membrane together with its full aqueous environment is a very ambitious one. The surface area typically occupied by the headgroup of such a lipid is of the order of magnitude of 100 $Å^2$. The amount of water necessary to simulate the wetting of a sufficiently large array of such headgroups is difficult to treat at the level of accuracy that we deem necessary here. The simultaneous treatment of the hydrophobic tails in the simulation is also difficult for the same reasons. Furthermore, at the present level of knowledge about intermolecular interaction potentials, little would be gained from setting up and studying a full system. Because of the lack of reliable and tested data available on the intermolecular interactions the interpretation of such simulation results would be quite uncertain.

We have thus chosen to study first a simplified model system consisting of two-dimensional arrays of deprotonated carboxilic acid headgroups in contact with water and hydrated Na^+ ions. The surface area occupied by a COO^- group is of the order of magnitude of 20 $Å^2$. This model system represents many of the important features associated with a membrane surface; similar systems are also studied experimentally (1–3). The COO^- groups are given translational and rotational mobility; the correlation of the translational motions of the headgroup with the ones of the first elements of the hydrophobic chain is incorporated in an effective way by increasing the mass of the carbon atom. The headgroups lead to a strong surface charge density. The structure of the liquid near the membrane will result from an interplay between the mutual influences of the headgroups, ionic charges, and the hydrogen bonded network structure of the bulk liquid. We have attempted to make our system large enough to be able to study the complete transition region from the membrane up to the bulk-like liquid phase.

As already stated, a useful interpretation of simula-

Address correspondence to Dr. Brickmann.

0006-3495/91/07/261/12 $2.00

tion results and the reduction of the observed phenomena to physical pictures as simple as possible is feasible only if the number of parameters involved (say the number of different atoms or molecules and the complexity of their mutual interactions) is not too high. Generally speaking, it is our goal to construct a simple model system for a membrane–aqueous medium interface with not too many parameters, which would allow to extract such typical features. Within this frame we attempt to model a typical system as realistically as possible, and for this reason we have selected molecules and groups for which the intermolecular interaction potentials are known with a high level of accuracy. The solvation of the Na^+ ion with the present model (V_{WW} and V_{WI}, vide infra Eq. 1) has for instance been studied in detail (4). A large body of comparative studies of results from simulations and experiments is available for aqueous ionic solutions in general (5–8). The interface between the model membrane used here and pure water has been studied separately (9, 10). It will serve here as a reference system when the influence of the ions is investigated.

Computer simulations are well suited for the study of complex systems like the present one, and many simulation studies of interfacial systems have been reported. As an example, the development of a two-dimensional hydrogen bond network in water in the vicinity of an uncharged platinum surface has recently been demonstrated (11). One-dimensionally hydrogen bonded water has been found and studied in model transmembrane channels (12). Other related simulation work dealt with micelles (13, 13*a*), inverted micelles (14) and cholesterol (15), mixtures of decanol and sodium-decanoate (16), phosphatidylcholine (17, 17*a*) interface regions, and, similar to the present case, Langmuir monolayers (18) and hexanol–water interfaces (19). These simulations can be subdivided into ones where the lipid surface is treated as an external potential (14, 17, 17*a*) and others with free moving lipid molecules. We shall demonstrate, as was also pointed out by other authors (13, 16), that the structure of the membrane surface is strongly influenced by the counterions. The influence of water on the motions of headgroups has been investigated previously (9). In this context we also note that analytical results for simpler, but similar, interfacial systems have recently become available (20). The molecular dynamics (MD) simulation method employed here allows in principle to determine both the static and the dynamic properties. In the present communications we shall restrict our attention mostly to the static or structural results.

The paper is organized as follows: first the interaction potentials and the simulation techniques used will be briefly discussed. After a short description of the evaluation techniques employed we shall discuss the stability of the model system. Then we shall consider the layering phenomenon observed in the water and in the ions in the vicinity of the membrane. The structure in these layers will be investigated next. In this context we stress again that we are presently not so much interested in exact quantitative results, but that we rather attempt to determine as unambiguously as possible typical features and trends. The ionic hydration shell will then be considered, and a few qualitative results concerning the approach of a hydrated ion toward the membrane will be presented.

II. INTERACTION POTENTIALS AND THE SIMULATIONS

The total intermolecular interaction potential energy is partitioned as a sum of molecule–molecule energies:

$$V^{tot} = V_{WW} + V_{WM} + V_{WI} + V_{MM} + V_{MI} + V_{II}, \qquad (1)$$

where the index W stands for a water molecule, M stands for a membrane COO^- group, and I stands for an ion. All terms in this sum are assumed to be sums of pairwise additive site–site potentials. The intramolecular geometries are kept rigid. The TIP4P (21) model is used for V_{WW}. V_{MM} results from a model by Jorgensen and Gao (22), this potential was also checked against various ab-initio calculations (23, 23*a*). With the help of combination rules (24) the potential V_{WM} is also determined; here we use the procedure of Lorentz–Berthelot. A detailed discussion and exploration of these potentials is given in reference 9. The Na^+ water interactions are described by a model fit to ab-initio data performed by Bounds and Bounds (25). The other interactions involving the Na^+ ion are modeled in terms of charged Lennard–Jones spheres and the combination rules are applied. For convenience, the functions describing all the pair potentials and other details of the models have been collected in an Appendix.

The simulated system consists of 60 COO^- groups representing two membrane surfaces limiting a central lamina with the liquid. The liquid consists of 859 water molecules and 60 Na^+ ions. The elementary box of the simulation is sketched in Fig. 1. The system is periodic in x- and y-direction. The composition of the system studied and other parameters of the simulation are given in Table 1. Cut-off radii similar to the ones used here have been used in related simulation work (13, 13*a*, 15, 19). Only two equations of motion are solved for the translations of the COO^- groups of the membranes in z-direction, i.e., only a collective motion of these groups is allowed in this direction. The individual COO^- groups

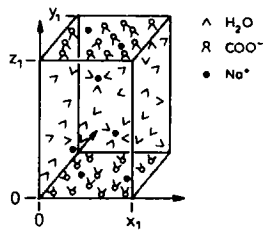

FIGURE 1 Elementary box. The two membrane surfaces are located at $z = 0$ and $z = z_1$. The system is periodic in x- and y-directions. The values for x_1 and y_1 and the average value for z_1 (see text) are given in Table 1.

can move in their x–y-plane and rotate around their axis of symmetry.

The arrangement in Fig. 1 is chosen mostly to obtain a sufficiently large number of averages. Furthermore, the presence of two independent membrane surfaces in the system allows to estimate the degree of statistical reliability reached by comparing the results obtained for the two halves of the box. Finally the problem of finding suitable boundary conditions for the bulk liquid is also avoided. The only prerequisite for this setup is the absence of direct interactions between the two surfaces.

The surface density of the COO^- groups is set to 0.05 $Å^{-2}$. The separation between the two surfaces, which was kept fixed in initial runs, is allowed to vary in the main run reported here. Starting from an equilibrated system with pure water between the two surfaces (9), the ions are introduced into the central zone of the lamina by exchanging water molecules. Before the ions are allowed to move, they are kept at fixed positions until hydration shells have developed. Four to eight ions are introduced at a time and the system is then allowed to reach a pseudoequilibrium state before the procedure is repeated. A small change in the water density, which is compensated by a volume shrinkage of the system, and which is due to the electrostriction of the water in the hydration shells of the Na^+ ions, is observed after each addition of ions. In a few instances a water molecule is pushed through the membrane surfaces by an ion. This did not lead to a loss of stability of the membrane. The total time during which ions are added is in excess of 150 ps.

TABLE 1 **Dimensions of the simulated system, number of particles, and other characteristic values of the simulation**

x_1	24.03 $Å$
y_1	24.97 $Å$
$\langle z_1 \rangle$	42.5 $Å$
n_{H_2O}	859
n_{COO^-}	60
n_{Na^+}	60
Timestep dt	0.5 fs
Simulation time t_{sim}	90 ps
Average temperature $\langle T \rangle$	297.5 K
Cut-off radius r_{cut} (Van der Waals)	7 $Å$
Cut-off radius r_{cut} (Coulomb)	11 $Å$

The main runs of the simulations reported here are carried out at a constant number of particles and total energy, but variable volume (see section IIIb). We did not observe any significant difference between the results of these runs and the ones obtained from ordinary NVE-MD. Further details of the simulation procedure are given in reference 9. During a typical run of 90 ps, the total energy remained constant to better than $\Delta E/E = 10^{-5}$ without rescaling of the velocities or other manipulations. The dynamical properties, such as transport coefficients or reorientation times, can thus be computed without corrections or adjustments, they will be reported in a forthcoming communication.

III. RESULTS

a. Methods of analysis

We shall discuss the water and hydration shell structures mainly by means of normalized atom–atom distance distribution functions $g_{\alpha\beta}(r_{\alpha\beta})$, where $r_{\alpha\beta}$ is the internuclear distance. The analysis of the water in the vicinity of the membranes is carried out by computing such functions separately for the different layers parallel to the membrane. In the case of homogeneous systems, this function is usually extended over the entire space around a particle (radial distribution function [RDF] or radial pair correlation function $h_{\alpha\beta}[r_{\alpha\beta}] = g_{\alpha\beta}[r_{\alpha\beta}] - 1$) and the integral

$$n_{\alpha\beta}(r_{\alpha\beta}) = 4\pi\rho_\beta \int_0^r g_{\alpha\beta}(r'_{\alpha\beta}) r'^2_{\alpha\beta} dr'_{\alpha\beta}, \qquad (2)$$

where ρ_β is the number density of species β in the system, is often called the running integration number. The value of this integral up to the first minimum of the g function is often referred to as the coordination number of species α by species β. If the minimum in the RDF is very shallow, it is obvious that this definition may not lead to very rigorous results (26). The plots presented here were generated from 6,000 configurations equally spaced throughout the simulation time of 90 ps. The peak heights and shapes did not depend on the bin size, which was varied between 0.02 and 0.04 Å. The curves were not smoothed.

The relative orientation between two molecules can in general be described by expansions of the generalized molecule–molecule pair correlation functions in terms of a set of invariant basis functions depending on the relative angles. In hydrogen-bonded liquids such expan-

sions tend to converge quite slowly even in homogeneous systems, and it is difficult to interpret the many resulting expansion coefficients. We have therefore chosen a simpler approach for the analysis in section IIIe.

b. Stability of the system

In initial runs of the series described above, the separation between the two membranes, and thus the total volume of the system, are adjusted in such a way as to obtain a density of ~ 1 g cm^{-3} in the center of the lamina. It was shown previously (9) that the structure of the liquid near the membrane is quite insensitive to the density in the center of the lamina. It is nevertheless of interest to explore whether this setup corresponds to an equilibrium state. To investigate this we have relaxed the constraint of constant separation between the two membranes imposed in earlier work (9) and solved two additional equations of motions in z-direction for the two membranes. The total mass of the 30 COO^- groups, including the enhanced masses of the carbon atoms, is used. Note that this system is not in equilibrium in a thermodynamic sense because, on one hand, there are no periodic boundary conditions in z-direction, and on the other, no external pressure is applied and no gas pressure can build up.

We found that after a short relaxation the separation between the two membranes oscillates with an amplitude of $\sim \pm 0.5$ Å and a frequency of < 10 cm^{-1} around an equilibrium. The density in the center of the lamina then oscillates around 1 g cm^{-3}. These slow anharmonic oscillations are not expected to couple with motions in the liquid or in the membranes. When more water molecules are exchanged for ions, the average separation of the membrane surfaces decreases slightly due to the electrostriction of the water in the hydration shells. The simulated system is thus stable at the time scale of the simulation. This is true even for systems containing less water than used here, i.e., with smaller average membrane–membrane separations.

The question of stability also arises with respect to the penetration of water or ions into the region outside the lamina. As was already mentioned above, water molecules are pushed through the membrane surface by ions approaching the membrane in a few instances; this did not destabilize the membrane. The water molecules usually attached to the positive end of the COO^- group and remained there for the duration of the simulation or reentered the lamina at a later time. During a total of more than 200 ps simulation with the maximum number of ions (sometimes even with less water molecules than in the main run reported here) we never observed the breakthrough of an ion.

In the case of pure water, a lowering of the density of the COO^- groups from 0.05 to 0.042 Å^{-2} was found to lead to massive breakthroughs of the water through the membrane. Repeating the same experiment in the presence of the Na^+ ions leads to similar results. We therefore restrict the present study to the aforementioned surface density of 0.05 Å^{-2}.

c. Layering of the liquid above the membrane

Fig. 2 shows the local density of the water molecule oxygens and hydrogens, averaged over the x- and y-coordinates, as a function of the distance from the plane of the carbon atoms of the COO^- groups. The resolution is 0.036 Å in the z-direction. For convenience, the curves are normalized by setting the number density of 0.0334 Å^{-3} for the oxygens and 0.0668 Å^{-3} for the hydrogens equal to the macroscopic water density of 1 g cm^{-3}. Results from the two membrane surfaces, see Fig. 1, are superimposed to show the degree of statistical reliability.

A layering of the water molecules extending 7–8 Å into the liquid is observed. The maximum density in the first layer is about three times the bulk density both for the oxygens and for the hydrogens. The average density of the oxygens between 2 and 3.1 Å from the reference plane is still enhanced by a factor of about two. This increase in average density is similar to the one found for pure water near the membrane, in spite of the fact that the details of the density fluctuations are different here. The shift between the oxygen and the hydrogen peaks in Fig. 2 is an indication of the average orientation of the

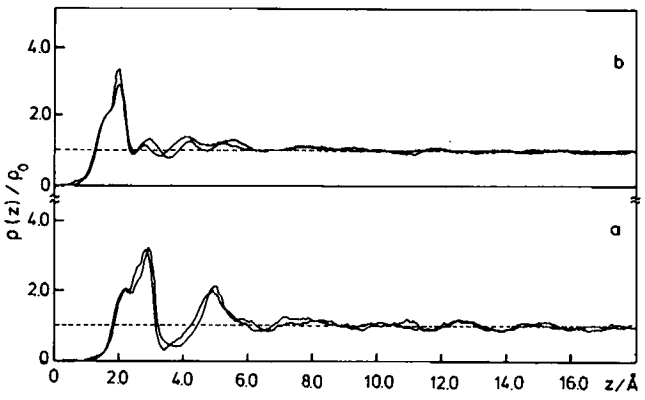

FIGURE 2 Local density of the water oxygens (a) and hydrogens (b) as functions of the distances from the plane of the carbon atoms. The curves obtained for the halves of the box (see Fig. 1) have been superimposed as a measure of the statistical reliability.

water molecules with respect to the surface normal of the membrane.

A second region of increased density is located between ~4.5 and 6 Å for the oxygens. Only washed-out features are found here for the hydrogens, indicating a loss of preferential orientation of the water molecules. Beyond 8 Å there are only small statistical oscillations in both curves so that this value can be taken as the upper limit of the influence of the membrane on the density of the ionic solution.

The local number density of the Na^+ ions is shown as a function of the distance from the reference plane in Fig. 3. Again the results obtained for the two halves of the box are superimposed. The fraction of the surface charge neutralized by Na^+ ions is also given as a function of the distance. A pronounced layer of ions is found in the immediate vicinity of the membrane, the integral over this peak is ~12.5. We thus find that <50% of the membrane charge is neutralized by cations in the first layer. This finding is in some contrast with results from analytical studies where very rapid charge neutralization (termed fast screening) is found (27).

Fig. 4 shows averaged density profiles for the Na^+ ions, analogue to Fig. 3, obtained during the process of addition of ions to the system. The results are for the pseudoequilibria reached after the ions have moved toward the membranes. They are averaged over time periods of ~25 ps each. It is seen that once there are enough ions in the system to complete the first layer, it remains stable. It is pushed toward the membrane surface, presumably by the buildup of the positive charge density of the cations being added to the system. In this process the layer becomes somewhat broader, but the number of Na^+ ions involved remains constant.

It is essential to consider both the effect of the electric charges and of the packing to understand these features. To create a favorable site for the adsorption of a cation on the membrane, the COO^- groups in the membrane must be orientated. It was shown previously (9) that the presence of pure water does not affect the structure of

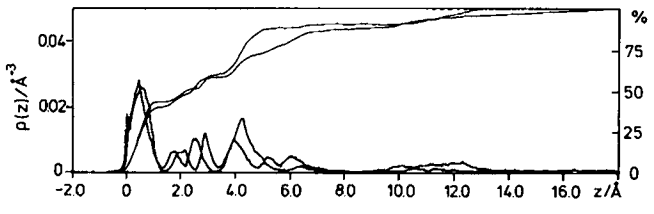

FIGURE 3 Local number density of the Na^+ atoms as a function of their distance from the plane of the carbon atoms. The percentage of the membrane charge neutralized is also given as a function of the distance from the membrane. The results for the two halves of the box are superimposed.

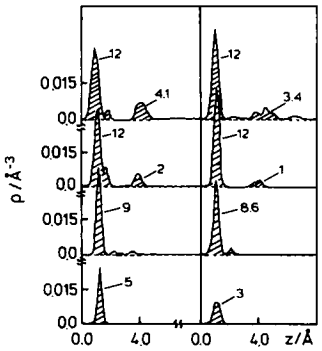

FIGURE 4 Local number density of the Na^+ ions, as in Fig. 3, for partially charged systems. Here the profiles obtained for the two membranes are shown separately. The numbers refer to the integrals over the peaks, i.e., to the number of Na^+ ions.

the membrane very much. This structure can be understood as a distorted hexagonal arrangement of the carbon atoms. The relative orientations of the O–O vectors of the COO^- groups is almost random in this case, with possibly a small preference for T-shaped configurations.

The local orientational order induced between the membrane groups by the ions is demonstrated in Fig. 5, which shows the normalized distance distribution functions for the oxygen- and carbon-atoms of the COO^- groups. They are contrasted with the same functions obtained in the absence of ions. Fig. 5 also shows the Na^+–Na^+ and Na^+–O (COO^-) normalized distance distribution. The typical distances found in the distribution functions in Fig. 5 are depicted in a sketch in Fig. 6.

The peak maximum of the ion density in Fig. 3 is at z = 0.5 Å, i.e., at the level of the oxygens. The positively charged ions attract the negative ends of the COO^- groups, leading to an environment of the ions with the O–O vectors of the COO^- groups preferentially oriented radially with respect to the ion. This condition can be fulfilled only for every second site on the membrane. In a very schematic picture the ions could be said to occupy positions of a 2 × 1 overlayer on bridge sites of a strongly distorted hexagonal surface. Characteristic chains –Na^+–O–O–Na^+–O–O– of such an overlayer can be identified in snapshot pictures of the membrane. Due to fluid-like behavior they are rather wavy. The idealized overlayer structure and a snapshot of an actual configuration are shown in Fig. 6 besides the sketch of an idealized Na^+ adsorption site on the membrane. The ions adsorbed at these sites are able to keep large parts of their hydration shells (vide infra). Other Na^+ ions are thus prevented from approaching the membrane, leading to the charge

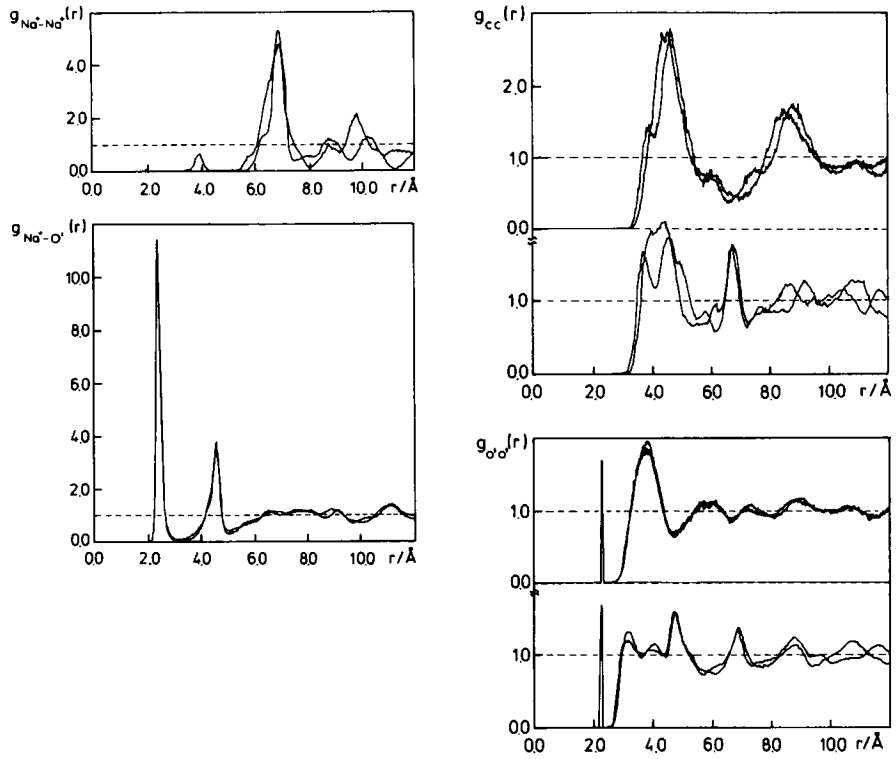

FIGURE 5 Normalized distance distribution functions $g_{Na^+-Na^+}$, $g_{Na^+-O'}$, and intermolecular part of g_{CC} and $g_{O'O'}$ for the COO^- groups. (O' is used for the oxygens here to avoid confusion with the water oxygens.) Results obtained in the absense of Na^+ ions are given for comparison (*upper curves*).

neutralization of $<50\%$ by this first layer, as described above.

Above the first layer of ions there is a diffuse region between ~ 1.7 and 3.7 Å. Approximately 5 Na^+ ions (per membrane surface) are found on the average in this region. A more pronounced second layer of ions can be identified around 4.25 Å. This layer contains about eight cations; some 85% of the membrane charge is thus neutralized within 5.5 Å from the plane of the carbons of the COO^- groups, taken here as reference. Ions in this layer are able to keep their full hydration shells. The remaining Na^+ ions are found throughout the lamina, where they seem to remain stable, at least at the time-scale of the simulation.

d. Structure in the liquid layers

The stratification of the liquid in layers parallel to the membrane is clearly established from Figs. 2 and 3. We have already discussed in some detail the structure of the layer of ions adsorbed directly on the membrane. The joint influence of the membrane and its ionic colayer on the water is the focus of interest in this section. For this purpose we define layers of 1-Å depth parallel to the membranes (see Table 2) for which normalized distance distribution functions have been computed separately. As a test, this procedure has formally also been used in the center of the lamina. If the liquid is homogeneous there, these distribution functions should become identical to the usual radial distribution functions. The literature values for this RDF (21) were also obtained from bulk TIP4P–water simulations, and the analysis in terms of layers was also tested on the bulk system.

Fig. 7 shows such oxygen–oxygen distance distribution functions obtained for layers, as defined in Table 2, parallel to the membrane. The influence of the membrane corrugation on the oxygen–oxygen order in the first layer is clearly visible. The oscillations in the distance distribution functions have a range of >10 Å, which is much larger than in liquid bulk water. With increasing distance from the membrane, the range of the ordering diminishes. Toward the center of lamina, i.e., at distances of >8 Å from the membranes, the functions here resemble more and more the usual RDF's obtained for bulk TIP4P–water under the same conditions. The main difference here is that first minimum and second maximum are somewhat less pronounced than in the bulk. It is also interesting to note that the transition between the structure in the first layers and the bulk

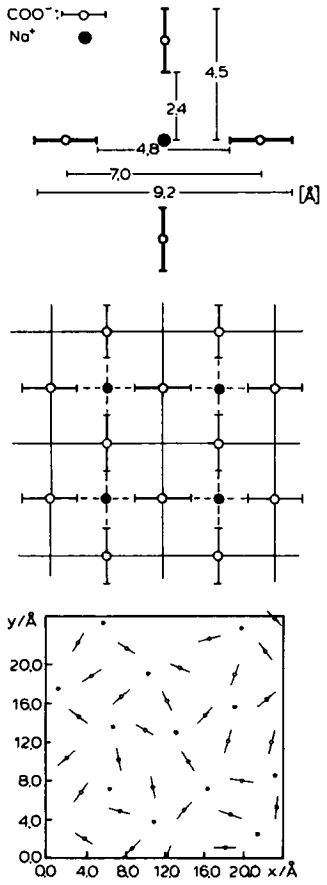

FIGURE 6 Sketch of a characteristic adsorption site of a Na^+ ion on the membrane with characteristic distances from the distance distribution functions in Fig. 5; sketch of the resulting idealized overlayer structure and snapshot of an actual configuration from the simulation.

structure seems to be a continuous one here, in contrast to the existence of a structure-broken region in the case of pure water (9). The transition region between surface induced structure and bulk structure is also narrower in the presence of ions.

Integrals analogue to the ones defined in Eq. 2, but

TABLE 2 Definition of the water and ion layers parallel to the membrane surfaces for the computation of the normalized distance distribution functions in Fig. 7

Layer	Water z/Å	Ion z/Å
1*a*	1.7–2.5	—
1*b*	2.5–3.3	—
1	1.9–2.9	0.0–1.0
2	4.4–5.4	3.5–4.5
3	6.9–7.9	—
4	11.9–12.9	—
5	15.0–16.0	—

Layers 1 *a* and 1 *b* are used in Fig. 9.

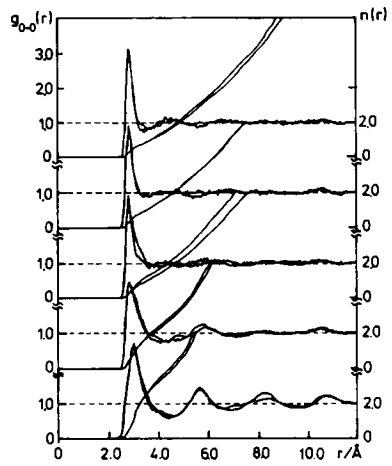

FIGURE 7 Normalized distance distribution functions of the water molecule oxygens in layers parallel to the membrane surface. From bottom to top: layers 1–5 as defined in Table 2.

extended here only over the layers of 1-Å thickness parallel to the membrane surface are also shown in Fig. 7. The value at the minimum between the first and second peak of the distribution function gives the mean number of next oxygen neighbors in the corresponding layer. In bulk water the integral extended over the entire next neighbor shell of a water molecule yields a value of slightly more than 4 (5), in keeping with to the predominantly tetrahedral environment of a molecule in the H-bond network. The mean number of next neighbors in a layer in bulk-like water in the center of the lamina is found to be 0.7. This is also the value to be expected from the total number of neighbors and the volume over which the integral is extended. The agreement of the value found in the simulation with the one statistically expected shows again that the structure in the center of the lamina is no longer influenced by the membranes. Close to the membrane, on the other hand, the number of next neighbors is increased to ~4.0 and 2.5 in the first and second water layer, respectively. This gives evidence for the destruction of the tetrahedral H-bond structure in the vicinity of the membrane.

The orientational order of the water molecules with respect to the membrane surfaces, which was already seen from the shift between the first peaks in the hydrogen and oxygen density profiles in Fig. 2, is studied in more detail by computing the average dipole moment of a water molecule in the z-direction $\langle \mu_z \rangle$. The Langevin parameter $a = \mu_0 E_z / k_B T$, where μ_0 is the dipole moment of the model TIP4P water (2.27 D), E_z is an equivalent electric field for the orientation of the water molecules, and the other symbols have their usual meaning, is

computed by means of the Langevin equation

$$\frac{\langle \mu_z \rangle}{\mu_0} = \coth(a) - \frac{1}{a}. \quad (3)$$

Fig. 8 shows the value of a as a function of the distance of the water molecule oxygen from the reference plane. Almost complete orientational order of the water dipoles with respect to the membrane surface normal is found at $z \approx 2$ Å. At smaller z values this orientational order decreases rapidly. Only a few water molecules penetrate into this region (cf. Fig. 2). In doing so, they tend to orient their dipoles with respect to the individual atoms of the COO^- groups rather than with respect to the membrane as a whole. Note also that due to the small number of molecules present these values have a large statistical uncertainty.

At distances larger than 2.5 Å the orientational order decreases toward a minimum, which coincides with the minimum in the oxygen density (see Fig. 2). A small second maximum is reached around 4 Å, which then decays slowly toward the center of the lamina. Similar to what was found for the density oscillations, the orientational order due to the membrane can be said to have vanished at distances above 8–10 Å. In keeping with the lower effective surface charge of the membrane together with the colayer of Na^+ ions, this range of the orientational order is shorter here than in the case of pure water. We recall that the average separation between the two membranes is 42.5 Å in the present system, thus allowing for a sufficiently large amount of water in the middle of the lamina not affected by the membranes.

e. Hydration of the Na^+ ion

The hydration structure of the Na^+ ion has been studied in many instances with different ion–water and water–water potentials. Single hydrated ions have been studied as well as salt solutions at different concentrations and pressures (5). It is generally concluded that the first hydration shell of this ion is well described by the available models, a detailed discussion can be found in the review literature cited above. At low to medium concentrations the coordination number according to the definition in Eq. 2 is found between 6 and 6.5.

Fig. 9 shows Na^+–O distance distribution functions between ions and water molecules in various layers. The first water layer (Table 2) has been subdivided here into two layers, labeled 1 a (shoulder close to the membrane, see Fig. 2) and 1 b (main peak). Two layers of ions are distinguished (see Table 2): layer one (0–1 Å) contains all ions directly adsorbed on the membrane and layer two (3.5–4.5 Å) consists of the ions forming the second pronounced peak at ~4 Å distance from the membrane. A bulk radial distribution function is included in Fig. 9

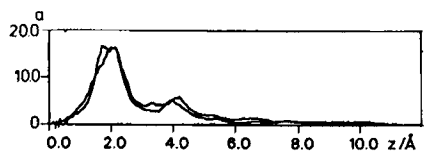

FIGURE 8 Parameter a of the Langevin function, see text, as a function of the distance between water molecule oxygens and the reference plane. Results for the two halves of the box are superimposed.

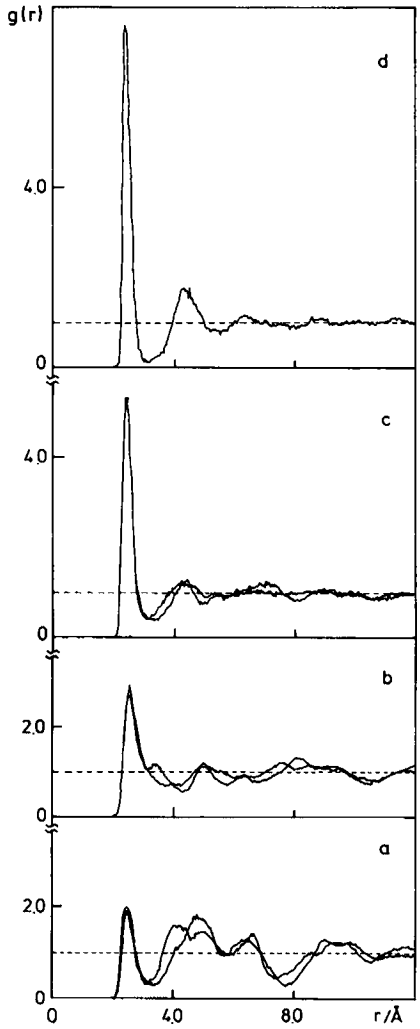

FIGURE 9 Na^+ oxygen distribution functions. From bottom to top: (a) Na^+ (1st layer), oxygen (layer 1 a); (b) Na^+ (1st layer), oxygen (layer 1 b); (c) Na^+ (2nd layer), oxygen (layer 2); (d) Na^+ (bulk), oxygen (bulk).

for comparison. Remarkable differences are seen in Fig. 9 between the various layers. With decreasing ion–membrane distance, the height of the first ion–oxygen peak decreases from 8 to ~2, while the position of this maximum shift from 2.37 to 2.52 Å. An increasingly pronounced long-range structure is simultaneously observed in these functions. The comparison of the Na^+ oxygen distribution functions for layers 1*a* and 1*b* shows a remarkably less pronounced first neighbor peak and an increased second neighbor peak for the water molecules in immediate vicinity of the membrane. This is a consequence of the decrease of ionic hydration because of hindrance by the COO^- groups at the membrane surface. The number of water molecules in the first hydration shells (i.e., within 3.2 Å from the ion) of first layer ions is ~2.2. About two-thirds of the first hydration shell is thus occupied by COO^- groups. For ions in the diffuse region between the first and second layers about one hydration water molecule is replaced by such a group. The ions in the second ion layer are completely hydrated. As a consequence of the increased water density their coordination number (7.1) is even higher than in bulk TIP4P water (6.3).

Distributions of relative orientations and the resulting averages are often used besides the distance distributions to characterize the ionic hydration. We calculate the average angle θ between the ion–oxygen vector and the dipole moments of the neighboring water molecules as a function of the ion–oxygen distance for ions and water molecules in the various layers. The potential energy minimum of the ion–water potential corresponds to $\theta = 0$. It is of special interest here to determine the range of the ion-induced order in the vicinity of the membrane. For this purpose we computed the difference between θ, as described above, and the mean orientation of the water molecules. This mean orientation θ_m is computed in the same way as θ but with respect to a large number of sites arbitrarily distributed in the layer. θ_m reflects the orientation of the molecules due to the membrane and the geometry factors resulting from the subdivision into layers. We then define an "excess" orientation $\theta_e = \theta_m - \theta$ of the water molecules with respect to the Na^+ ions.

Fig. 10 shows θ, θ_m, and θ_e as functions of the site–oxygen distance for different ion and water layers (layer definitions from Table 2). As a convenient measure of the influence of the membrane interface on the hydration shell orientation we chose the value of θ at an ion–oxygen distance of 2.4 Å. At this distance θ has its best statistical reliability because it corresponds roughly to the first peak of the Na^+ oxygen pair distribution function. The values are 102, 58, and 40 degrees in the first and second layers and in bulk water, respectively.

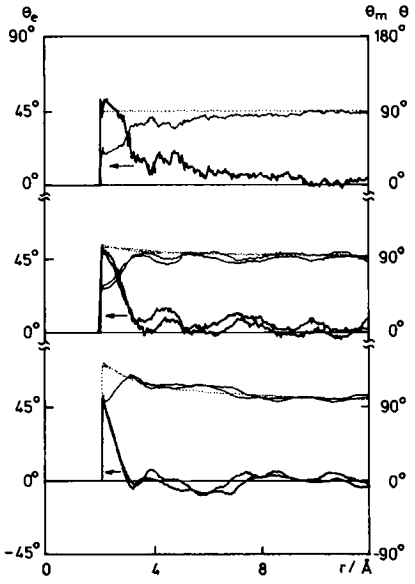

FIGURE 10 Angles Θ, thin lines, Θ_m, dotted lines (*right scale*), and Θ_e, fat lines (*left scale*), as defined in the text, as functions of the site (ion)-oxygen distance. (*Bottom*) Ion (layer 1), water (layer 1); (*middle*) Ion (layer 2), water (layer 2); (*top*) bulk. Ion layers as in Fig. 9.

This shows that even the average orientation in the first hydration shell of a sodium ion is considerably disturbed in the vicinity of the membrane (recall that the ion–water potential energy minimum corresponds to $\theta = 0$). The curves θ_e show the range of ion-induced orientational order. All three curves show a region of strong excess orientation which reaches up to a distance of ~3.2 Å. This distance corresponds to the outer limit of the first hydration sphere as defined by the Na^+–O pair distribution function (Fig. 9). In the case of a sodium ion in bulk water this region is followed by a second one of increased orientation which extends to ~5.5 Å and coincides with the second hydration sphere at the top of Fig. 9. As seen in the middle and the bottom of Fig. 10, this orientational influence in the region of the second hydration sphere is increasingly suppressed in the course of approach to the membrane surface.

f. Approach of a hydrated Na^+ ion toward the membrane

As described above, the ions are introduced into the system by exchanging water molecules near the center of the lamina. They are immobilized until a hydration shell has formed and then allowed to move. After some time the ions start accelerating toward one of the membrane surfaces, dragging along their hydration shells, or at least large parts of them. We have used these events to

obtain a qualitative picture of the microscopic events during the approach of a hydrated ion toward a charged membrane. A major point of interest here is, for instance, the stripping of the hydration shell off the ion before entering a transmembrane channel.

The representation in Figs. 11 has been chosen to get a picture independent of the velocity of the ion approaching the membrane. Fig. 11 *a* shows the distance that a water molecule travels attached to a Na^+ ion approaching the surface. Attachment to the ion is defined here as follows: a water molecule is considered to be attached to an ion after having approached closer than $R_2 = 2.77$ Å. It is considered detached again if its separation from the ion becomes larger than $R_3 = 3.92$ Å. R_n is the distance at which the ion–oxygen RDF is equal to one for the nth time. This somewhat cumbersome definition is necessary to omit oscillatory motions of water molecules entering and leaving the hydration shell from the statistics. The abscissa in Fig. 11 *a* gives the distance from the membrane at which a water molecule enters the hydration shell for the first time. The ordinate is the distance from the surface. We have drawn vertical lines for each water molecule belonging to a hydration shell starting from the location where it entered the shell to the location where it left it. The lines below the diagonal thus belong to molecules which accompany the ion over a certain distance toward the membrane. Lines above the diagonal are molecules which enter the hydration shell "in front" of a moving ion and leave it after having been "pushed aside" and rotated around the ion. At small ion–surface distances the water molecules that are pushed through the surface (see section IIIb) are seen. Average distances are shown in the lower part of the graph. It shows again that the distance that water molecules travel attached to an ion decreases markedly with decreasing distance from the surface. Below 5 Å the ion moves toward the membrane essentially without dragging along any water.

Fig. 11 *b* is an analogue graph. It shows a vertical line for each water molecule attached to an ion. Here the abscissa gives the position of the ion above the membrane at the time the water molecule attached. The line extends from there to the position of the ion at the time when the water molecule left the hydration shell. From this figure it is seen that the distance a given ion travels attached to a certain water molecule is on the average longer than the distance covered by the water, Fig. 11 *a*. This suggests a mechanism where water molecules enter the hydration shell predominantly "in front" of the ion, are pushed aside and eventually dragged along for a certain distance in a rotative movement around the ion, and then leave the hydration shell "behind" the ion. This effect is particularly clear at distances below 5 Å.

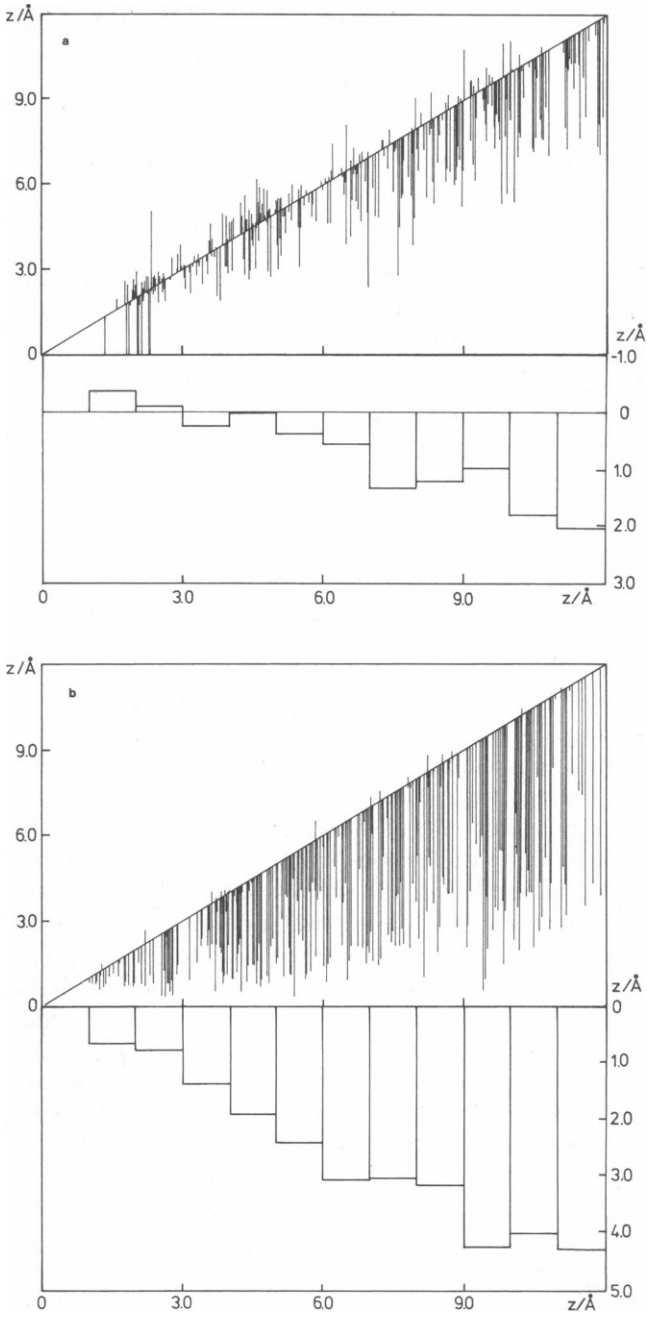

FIGURE 11 Illustration of the dynamics in the hydration shells of Na^+ ions approaching the membrane surface. (*a*) Distances that water molecules travel attached to ions as a function of the distance of the water molecule from the membrane where the attachment occurred (*upper part, left scale*), and values averaged over 1 Å (*lower part, right scale*); (*b*) distances that ions travel attached to a given water molecule as a function of the distance of the ion from the membrane where the attachment occured (*upper part, left scale*) and values averaged over 1 Å (*lower part, right scale*).

IV. SUMMARY AND CONCLUSIONS

The main results of the present investigation can be summarized as follows: the overall influence of a membrane surface consisting of deprotonized carboxilic headgroups extends ~8 Å into an aqueous solution. In this region remarkable structural changes are found compared with pure liquid. The average density is, for instance, strongly increased in the vicinity of the surface. Furthermore, only ~50% of the membrane charge is neutralized by counterions in the first adsorbed layer. This is a consequence of the headgroup mobility. Ions in the first layer above the membrane lose a part of their hydration shells and are coordinated by headgroups, forming a kind of overlayer. Further ions are prevented to enter into this region once the overlayer is formed. Presently we prepare and simulate more realistic model systems with larger headgroups and also include the hydrophobic tails.

APPENDIX

Intermolecular interaction potentials (energies in 10^{-21} J, distances in Å) and other details of the models

$$V_{WW} = v_{OO} + v_{mm} + \sum_{i=1,2} v_{mH_i} + \sum_{i,j=1,2} v_{H_iH_j}$$

$$v_{OO} = 4.308 \cdot \left[\left(\frac{3.154}{r_{OO}}\right)^{12} - \left(\frac{3.154}{r_{OO}}\right)^{6}\right]$$

$$v_{mm} = \frac{2.495 \cdot 10^3}{r_{mm}}$$

$$v_{mH} = \frac{-1.248 \cdot 10^3}{r_{mH}}$$

$$v_{HH} = \frac{6.238 \cdot 10^2}{r_{HH}}.$$

The (fixed) intramolecular O–H distance is 0.9572 Å, the H–O–H angle is 104.5°. The point m is located on the H–O–H angle bisector at a distance of 0.15 Å from the oxygen. The partial charges leading are +0.52 e on the hydrogens and −1.04 e on point m.

$$V_{WM} = \sum_{i=1,2} v_{OO'_i} + \sum_{i=1,2} v_{mO'_i} + \sum_{i,j=1,2} v_{H_jO'_i} + v_{OC} + v_{mC} + \sum_{i=1,2} v_{H_iC}$$

$$v_{OO'} = 5.016 \cdot \left[\left(\frac{3.057}{r_{OO'}}\right)^{12} - \left(\frac{3.057}{r_{OO'}}\right)^{6}\right]$$

$$v_{mO'} = \frac{1.800 \cdot 10^3}{r_{mO'}}$$

$$v_{HO'} = \frac{-8.998 \cdot 10^2}{r_{HO'}}$$

$$v_{OC} = 3.713 \cdot \left[\left(\frac{3.477}{r_{OC}}\right)^{12} - \left(\frac{3.477}{r_{OC}}\right)^{6}\right]$$

$$v_{mC} = \frac{-1.200 \cdot 10^3}{r_{mC}}$$

$$v_{HC} = \frac{5.999 \cdot 10^2}{r_{HC}}.$$

Here O′ refers to the oxygen on the COO^- group.

$$V_{MM} = v_{CC} + \sum_{i,j=1,2} v_{O'_iO'_j} + \sum_{i=1,2} v_{CO'_i}$$

$$v_{CC} = \frac{5.768 \cdot 10^2}{r_{CC}} + 3.196 \cdot \left[\left(\frac{3.800}{r_{CC}}\right)^{12} - \left(\frac{3.800}{r_{CC}}\right)^{6}\right]$$

$$v_{O'O'} = \frac{1.298 \cdot 10^3}{r_{O'O'}} + 5.836 \cdot \left[\left(\frac{2.960}{r_{O'O'}}\right)^{12} - \left(\frac{2.960}{r_{O'O'}}\right)^{6}\right]$$

$$v_{CO'} = \frac{-8.652 \cdot 10^2}{r_{CO'}} + 4.319 \cdot \left[\left(\frac{3.380}{r_{CO'}}\right)^{12} - \left(\frac{3.380}{r_{CO'}}\right)^{6}\right].$$

The intramolecular geometry of the COO^- group is also kept fixed, the C–O′ distance is 1.231 Å and the O′–C–O′ angle is 131°. The partial charges are +0.50 e on the carbon atom and −0.75 e on the oxygen. A mass of 54 a.u. is located at the position of the carbon to mimic the first elements of the hydrophobic chain.

$$V_{WI} = v_{OI} + v_{mI} + \sum_{i=1,2} v_{H_iI}$$

$$v_{OI} = 1.900 \cdot 10^5 \cdot e^{-3.546 \cdot r_{OI}} - \frac{3.022 \cdot 10^3}{r_{OI}^4} + \frac{5.836 \cdot 10^3}{r_{OI}^6}$$

$$v_{mI} = \frac{-2.399 \cdot 10^3}{r_{mI}}$$

$$v_{HI} = 1.434 \cdot 10^4 \cdot e^{-3.394 \cdot r_{HI}} + \frac{1.200 \cdot 10^3}{r_{HI}}$$

$$V_{MI} = v_{CI} + \sum_{i=1,2} v_{O'_iI}$$

$$v_{CI} = \frac{1.154 \cdot 10^3}{r_{CI}} + 2.756 \cdot \left[\left(\frac{3.265}{r_{CI}}\right)^{12} - \left(\frac{3.265}{r_{CI}}\right)^{6}\right]$$

$$v_{O'I} = \frac{-1.730 \cdot 10^3}{r_{O'I}} + 3.724 \cdot \left[\left(\frac{2.845}{r_{O'I}}\right)^{12} - \left(\frac{2.845}{r_{O'I}}\right)^{6}\right]$$

$$V_{II} = \frac{2.307 \cdot 10^3}{r_{II}} + 2.376 \cdot \left[\left(\frac{2.730}{r_{II}}\right)^{12} - \left(\frac{2.730}{r_{CI}}\right)^{6}\right].$$

We thank the Höchstleistungsrechenzentrum (HLRZ) at the Forschungsanlage Jülich (KFA) for a grant of computer time on their CRAY X-MP and later on CRAY Y-MP. We also thank the Rechenzentrum der Technischen Hochschule Darmstadt for computer time on the IBM 3090 VF.

Support by the Deutsche Forschungsgemeinschaft and by the Fonds der Chemischen Industrie is gratefully acknowledged. Dr. Bopp also thanks the Deutsche Forschungsgemeinschaft for the award of a Heisenberg fellowship.

Received for publication 5 November 1990 and in final form 25 February 1991.

REFERENCES

1. Laxhuber, L. A., and H. Möhwald. 1987. Thermodesorption spectroscopy of Langmuir-Blodgett films. *Langmuir.* 3:837–845.
2. Joosten, J. G. H. 1988. Light scattering from thin liquid films. *In* Thin Liquid Films. I. B. Ivanow, editor. Marcel Dekker Inc., New York. 569–662.
3. Gaines, G. L. 1966. Insoluble Monolayers at Liquid-Gas Interfaces. Interscience Monographs on Physical Chemistry, New York.
4. Bounds, D. G. 1985. A molecular dynamics study of the structure of water around Li^+, Na^+, K^+, Ca^{++}, Ni^{++}, and Cl^-. *Mol. Phys.* 54:1335–1355.
5. Bopp, P. 1987. Molecular dynamics simulations of aqueous ionic solutions. *In* The Physics and Chemistry of Aqueous Ionic Solutions. M-C. Bellissent-Funel and G. W. Neilson, editors. Reidel, Boston, MA. 217–243.
6. Heinzinger, K. 1990. Molecular dynamics simulations of aqueous systems. *In* Computer Modelling of Fluids, Polymers and Solids. C. R. A. Catlow et al., editors. Kluwer Academic Publishers, Dordrecht, the Netherlands. 357–394.
7. Bopp, P. 1989. Molecular dynamics computer simulations of hydrogen-bonded liquids. *In* Intermolecular Forces—An Introduction to Modern Methods and Results. P. Huyskens, W. A. P. Luck, and Th. Zeegers-Huyskens, editors. Springer Verlag, New York. In press.
8. Enderby, J. 1987. The Physics and Chemistry of Aqueous Ionic Solutions. M-C. Bellissent-Funel and G. W. Neilson, editors. Reidel, Boston, MA. 129–145.
9. Schlenkrich, M., K. Nicklas, J. Brickmann, and P. Bopp. 1989. A Molecular Dynamics Study of the Interface between a Membrane and Water. *Ber. Bunsen. Phys. Chem.* 94:133–145.
10. Schlenkrich, M., P. Bopp, M. Knoblauch, A. Skerra, and J. Brickmann. 1988. Molecular dynamics simulations on the role of water for the ion transports through narrow transmembrane channels. *In* Advances in Biotechnology of Membrane Ion Transport. P. L. Jorgensen and R. Varna, editors. Serono Symposia Publications, Raven Press, New York. 51:135–146.
11. Spohr, E., 1989 Computer simulations of the water/platinum interface. *J. Phys. Chem.* 93:6171–6180.
12. Skerra A., and J. Brickmann. 1987. Structure and dynamics of one-dimensional solutions in biological transmembrane channels. *Biophys. J.* 51:969–976.
13. Jönsson B., O. Edholm, and O. Teleman. 1986. Molecular dynamics simulations of a sodium octanoate micelle in aqueous solution. *J. Chem. Phys.* 85:2259–2271.

13a. Watanabe, K., M. Ferrario, and M. L. Klein. 1988. Molecular dynamics study of a sodium octanoate micelle in aqueous solution. *J. Phys. Chem.* 92:819–821.

14. Linse, P. 1989. Molecular dynamics study of the aqueous core of a reversed ionic micelle. *J. Chem. Phys.* 90:4992–5004.
15. Engelmann, A. R., C. Medina Llanos, P. G. Nyholm, O. Tapia, and I. Pascher. 1987. Studies on membrane hydration. Part I. Monte Carlo simulation of the cholesterol-water interface. *J. Mol. Struct.* 151:81–102.
16. Egberts E., and H. J. C. Berendsen. 1988. Molecular dynamics simulation of a smectic liquid crystal with atomic detail. *J. Chem. Phys.* 89:3718–3732.
17. Scott, H. L. 1985. Monte Carlo studies of liquid/water interfaces. *Biochim. Biophys. Acta.* 814:327–332.

17a. Hussin, A., and H. L. Scott. 1987. Density and bonding of interbilayer water as functions of bilayer separation: a Monte Carlo study. *Biochimica et Biophysica Acta.* 897:423–430.

18. Chuiko, A. A., V. Ya. Antonchenko, V. V. Ilyin, N. N. Makovsky, and V. M. Ogenko. 1990. Molecular mechanism of Langmuir monolayer "sliding" off water surface. *Academy of Sciences of the Ukranian SSR, Institute of Theoretical Physics preprint.* ITP-90-57E.
19. Gao J., and W. L. Jorgensen. 1988. Theoretical examination of hexonal-water interfaces. *J. Phys. Chem.* 92:5813–5822.
20. Torrie, G. M., A. Perera, and G. N. Pattey. 1989. Reference hypernetted chain theory for hard spheres at charged surfaces. *Mol. Phys.* 67:1337–1353.
21. Jorgensen, W. L., J. Chandrasekhar, J. D. Madura, R. W. Impey, and M. L. Klein. 1983. Comparison of simple potential functions for simulation of liquid water. *J. Chem. Phys.* 79:926–935.
22. Jorgensen, W. L., and J. Gao. 1986. Monte Carlo simulations of the hydration of ammonium and carboxylate ions. *J. Phys. Chem.* 90:2174–2182.
23. Lukovits I., A. Karpfen, H. Lischka, and P. Schuster. 1979. Ab initio studies on the hydration of formate ion. *Chem. Phys. Lett.* 63:151–154.

23a. Berthod, H., and A. Pullmann. 1981. Molecular potential, cation binding, and hydration properties of the carboxylate anion. Ab initio studies with an extended polarization basis set. *J. Comput. Chem.* 2:87–95.

24. Wiese, H., and J. Brickmann. 1989. Lennard-Jones (12,6) potentials for the nonionic interactions of alkali cations and halide anions—a test of different combination rules. *Ber. Gunsenges. Phys. Chem.* 93:1464–1467.
25. Bounds, D. J., and P. J. Bounds. 1983. Potential surface derived from gradient calculations. New potentials for Li^+/H_2O, Na^+/H_2O, and K^+/H_2O. *Mol. Phys.* 50:25–32.
26. Heinzinger, K., P. Bopp, and G. Jancsó. 1986. Molecular dynamics simulation of ionic hydration. *Acta Chimica Hungarica.* 121:27–53.
27. Torrie, G. M., P. G. Kusalik, and G. N. Patey. 1989. Molecular solvent model for an electric double layer: reference hypernetted chain results for potassium chloride solutions. *J. Chem. Phys.* 90:4513–4527.